J. Membrane Biol. 47, 327–355 (1979)

Intracellular Sodium Activity and Sodium Transport in *Necturus* Gallbladder Epithelium

J. Graf* and G. Giebisch

Yale University School of Medicine, 333 Cedar Street, New Haven, Connecticut 06510

Received 4 August 1978; revised 26 January 1979

Summary. Ion-sensitive glass microelectrodes, conventional microelectrodes and isotope flux measurements were employed in *Necturus* gallbladder epithelium to study intracellular sodium activity, $[Na]_i$, electrical parameters of epithelial cells, and properties of active sodium transport. Mean control values were: $[Na]_i$: 9.2 to 12.1 mM; transepithelial potential difference, Ψ_{ms}: -1.5 mV (lumen negative); basolateral cell membrane potential, Ψ_{cs}: -62 mV (cell interior negative); sodium conductance of the luminal cell membrane, g_{Na}: 12 μmho cm^{-2}; active transcellular sodium flux, 88 to 101 pmol cm^{-2} sec^{-1} (estimated as instantaneous short-circuit current). Replacement of luminal Na by K led to a decrease of the intracellular sodium activity at a rate commensurate to the rate of active sodium extrusion across the basolateral cell membrane. Mucosal application of amphotericin B resulted in an increase of the luminal membrane conductance, a rise of intracellular sodium activity, and an increase of short-circuit current and unidirectional mucosa to serosa sodium flux. Conclusions: (i) sodium transport across the basolateral membrane can proceed against a steeper chemical potential difference at a higher rate than encountered under control conditions; (ii) the luminal Na-conductance is too low to accommodate sodium influx at the rate of active basolateral sodium extrusion, suggesting involvement of an electrically silent luminal transport mechanism; (iii) sodium entry across the luminal membrane is the rate-limiting step of transcellular sodium transport and active sodium extrusion across the basolateral cell membrane is not saturated under control conditions.

Sodium movement across epithelial membranes occur along both a cellular and a paracellular pathway. In "leaky" epithelia such as that of the gallbladder, passive transport across the paracellular shunt pathway is the dominating factor in determining the overall transepithelial ion permeability. In contrast, the rate of active transcellular transport of sodium is determined by two sequential operations: by the rate of sodium entry across the luminal membrane, be it by diffusion down an

* *Present address:* University of Vienna, Department of General and Experimental Pathology, Wahringerstraße 13, A-1090 Vienna, Austria.

0022-2631/79/0047-0327 $05.80

electrochemical gradient or mediated by a specific carrier, and by active extrusion of sodium ions across the basolateral cell membrane by an electroneutral or rheogenic pump mechanism.

The existence of a relatively low resistance paracellular shunt pathway has been clearly demonstrated for *Necturus* gallbladder epithelium (Frömter, 1972, Frömter & Diamond, 1972), and further advances in our understanding of the mechanisms of cellular sodium transport were made by Reuss and Finn (1975*a*, *b*) and van Os and Slegers (1975), who studied the permeability properties of the luminal and basolateral cell membranes. Several investigators have succeeded in using ion-sensitive microelectrodes to measure intracellular sodium activity in sodium transporting epithelia (Lee & Armstrong, 1972; Zeuthen & Monge, 1975), including *Necturus* gallbladder (Zeuthen, 1976, 1977).

In the present study measurements of intracellular sodium activities and of transepithelial transport were carried out under conditions of reduced and enhanced sodium entry across the luminal cell membrane. Reduction of sodium entry was achieved by abolishing its electrochemical gradient across the luminal membrane. This resulted in a rapid fall of the intracellular sodium concentration. On the other hand, increasing the permeability of the luminal membrane by amphotericin B led to a sharp rise of the intracellular sodium activity with a simultaneous increase of the transepithelial sodium transport and the transepithelial electric potential. Comparison of these results with electrophysiological parameters obtained in this and other studies (Reuss & Finn, 1975*a*, *b*) shows that: (i) the sodium pump of the basolateral membrane is rheogenic, at least under conditions of an increased load; (ii) the intracellular sodium activity determines the pumping rate and that the sodium pump is not saturated under control conditions; (iii) sodium entry across the luminal membrane is the rate-limiting step of transepithelial sodium transport; and (iv) it is unlikely that diffusion of sodium ions is the sole mechanism for its translocation across the luminal cell membrane.

Materials and Methods

The experiments were carried out on isolated gallbladders of *Necturus maculosus* (Lemberger Co., Oshkosh, Wisc.). Effects of ionic replacements were studied during July to October, those of amphotericin B (Fungizone, E.R., Squibb & Sons) in November and December.

The animals were anesthetized by immersion in a solution of tricaine methansulfonate in tap water (660 mg/liter). After disappearance of cutaneous reflexes the abdo-

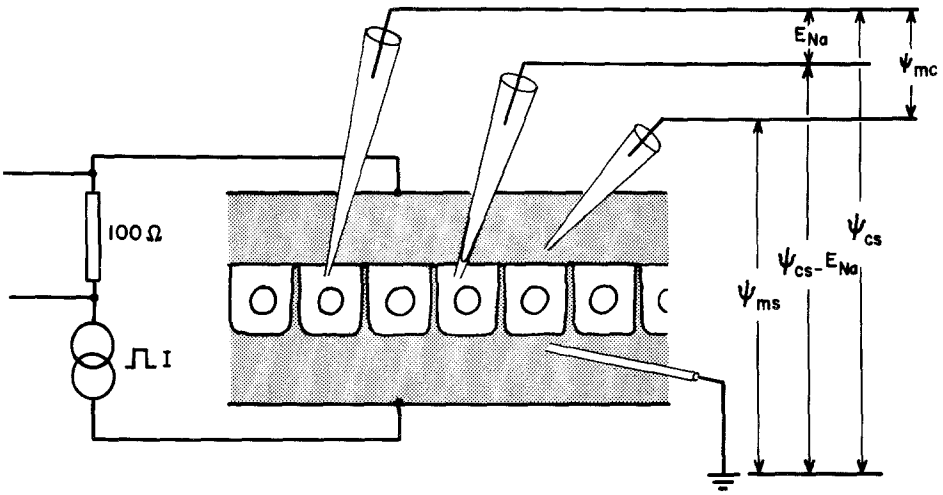

Fig. 1. Electrode arrangement for the measurement of electrical parameters and of intracellular sodium activity in *Necturus* gallbladder epithelium. The gallbladder was mounted as a flat sheet between two current-passing electrodes. Cells were impaled from the mucosal surface with Ling-Gerard and sodium-sensitive glass microelectrodes. Potentials were recorded with reference to the serosal or mucosal (not shown) bathing solution or by electronic subtraction as indicated. Ψ_{cs}; serosal membrane potential; Ψ_{mc}; mucosal membrane potential; E_{Na}; intracellular sodium potential (with reference to the extracellular value determined before impalement). Changes of Ψ_{ms}, Ψ_{mc}, and Ψ_{cs} due to transepithelial current were used to determine R_{te} (transepithelial resistance) and r (voltage divider ratio)

minal cavity was opened by a median incision, the gallbladder was removed, cleaned from adhering liver tissue, emptied, and cut longitudinally. After washing it free from bile residues in amphibian Ringer's solution, it was mounted as a flat sheet in a slightly modified Ussing-type perfusion chamber similar to the one used by Frömter (1972). The exposed tissue area was 0.5 cm^2; the fluid inlet of the lower (serosal) chamber (volume 1 ml) was located at the bottom and accommodated one current-passing Ag–AgCl electrode. A fluid outlet was placed 1 mm below the supporting grid of the tissue and the waste fluid passed a flowing KCl–Ag–AgCl electrode connected to ground. The upper (mucosal) chamber contained a circular Ag–AgCl current electrode. The transepithelial potential was measured with reference to ground by a Ringer-agar–KCl–Ag–AgCl electrode in the mucosal bath, or when changes of the ion concentrations were applied, by a low resistance Ling-Gerard type electrode filled with 3 M KCl. The mucosal bath was changed periodically by suction and refilling with different oxygenated solutions. All experiments were carried out at room temperature.

The standard perfusion solution contained (mM): NaCl, 90; KCl, 2.5; $CaCl_2$, 1.8; $MgCl_2$, 1.0; $NaHCO_3$, 10.0; NaH_2PO_4, 0.5; pH 7.74, gassed with 99% O_2, 1% CO_2; sodium activity in the control solution is calculated to be 78.4 mM/liter; in some experiments NaCl was replaced isotonically by KCl or raffinose.

Epithelial cells were impaled from the mucosal side under visual control (Leitz TS stereomicroscope) with bevelled microelectrodes (Brown & Flaming, 1974) filled with 3 M KCl and with a sodium-sensitive recessed-type glass microelectrode (Thomas, 1972). The KCl-filled microelectrodes were connected via Ag–AgCl electrode holders to an M 701

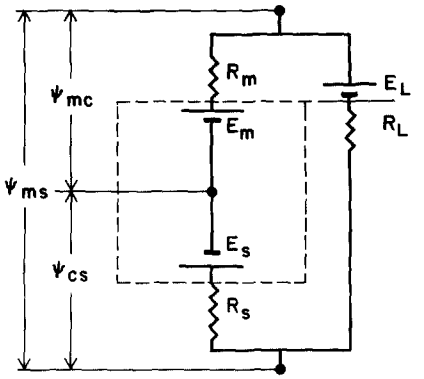

1) MUCOSAL MEMBRANE POTENTIAL

$$\psi_{mc} = \frac{E_m(R_s+R_L) + R_m(E_s+E_L)}{R_m+R_s+R_L}$$

2) TRANSEPITHELIAL POTENTIAL

$$\psi_{ms} = \frac{E_L(R_m+R_s) + R_L(E_m-E_s)}{R_m+R_s+R_L}$$

3) VOLTAGE DIVIDER RATIO

$$r = \frac{\Delta\psi_{mc}}{\Delta\psi_{cs}} = \frac{R_m}{R_s}$$

4) TRANSEPITHELIAL CONDUCTANCE

$$\frac{1}{R_{te}} = \frac{1}{R_L} + \frac{1}{R_m+R_s}$$

or:

$$E_m = \frac{\psi_{mc}(R_m+R_s) - R_m(\psi_{ms}+E_s)}{R_s}$$

$$E_s = \frac{\psi_{mc}R_L - \psi_{ms}(R_s+R_L) + E_L R_s}{R_L}$$

$$E_L = \frac{\psi_{ms}(R_s+R_L) + R_L(E_s-\psi_{mc})}{R_s}$$

Fig. 2. Equivalent circuit of gallbladder epithelium used to determine electromotive forces and resistances of the mucosal membrane (E_m, R_m), the serosal membrane (E_s, R_s) and the lateral paracellular shunt (E_L, R_L) by the equations given below

amplifier (WP-Instruments, Hamden, Conn.), and the sodium-sensitive electrodes to a high impedence electrometer (F-23, WP-Instruments, Hamden, Conn.). The electrode arrangement and the circuit diagram are shown in Fig. 1, and Fig. 2 shows the equivalent circuit and some of the equations used to assess various circuit parameters. Cells were impaled by advancing the microelectrode towards the cell membrane until an increase of noise (and electrode resistance) and a small, usually positive, potential change was observed. The electrode was advanced and the membrane punctured by cautiously tapping the table. Stable potential readings were most frequently obtained when the impalement resulted in a step voltage change and not in a transient overshoot or gradual potential increase.

The transepithelial potential, Ψ_{ms}, is given with reference to the serosal bathing solution. The basolateral (serosal) cell membrane potential, Ψ_{cs}, is also referred to the serosal bathing solution, and the apical (mucosal) cell membrane potential, Ψ_{mc}, is the

potential of the mucosal bathing solution with reference to the intracellular potential. The same sign convention is used to describe the respective emf's, E_L, E_S and E_M.

The transepithelial resistance (R_{te}) and the "voltage divider ratio" (r, Rm/Rs) were measured by passing 300 msec rectangular current pulses between the mucosal and serosal current electrodes from a floating constant current source. Current was measured by the voltage drop across a 100 Ω resistor by means of a differential electrometer amplifier.

The mucosal potential recording electrode was placed in immediate proximity to the epithelium. Correction both for a small resistance of the serosal connective tissue and the 1-mm serosal fluid (20–25 ohm cm^2) was made by scraping off the epithelium at the end of each experiment. A value of 16.5 ohm cm^2 was obtained by Fromm *et al.* (1977) for the subepithelial connective tissue in *Necturus* gallbladder.

Sodium-sensitive glass microelectrodes were constructed from Corning NAS 11.18 glass as described by Thomas (1972), an effort being made to achieve a very small volume of the recess in the tip (100–200 μm^3). The electrodes were bevelled under microscopic control on a rotating (approx. 1 cps) optical flat glass disc, covered with a polyurethane film, and sprayed with 0.1 μm alumina particles as grinding abrasive (Brown & Flaming 1975). Electrodes with a just visible opening at the tip (approx. 0.5 μm) gave stable impalements and a relatively fast reading of changes of the sodium concentration (90% of the full response in 1 to 5 min). The electrodes were calibrated in Ringer's solutions of different sodium concentrations, sodium being replaced by equivalent amounts of potassium (Na^+, 100–10 mM; K^+, 2.5–92.5 mM). This procedure was chosen to avoid significant changes in ionic strength and to approach a cationic environment similar to that of cell fluid. Electrode resistances were estimated by shunting their emf in sodium-containing media through a 10^9 Ω resistor and measuring the remaining voltage drop. Electrodes were accepted if they gave a response of 55–56 mV for a tenfold change of the sodium concentration, exhibiting a selectivity of Na over K better than 70:1. The electrodes had thus quite similar characteristics as those described by Thomas (1976). These electrodes had resistances of $>8 \times 10^{10}$ Ω. Intracellular sodium activities, $[Na^+]_i$, were calculated from the activity coefficient of the Ringer's solution (0.78), and the nonideal slope of the sodium electrode as given above. The chemical potential difference between intracellular fluid and bathing solution is given as E_{Na}.

Mucosa to serosa sodium flux (J_{ms}^{Na}) was measured with ^{24}Na containing Ringer's solution in the mucosal chamber. The effluent of the serosal chamber was collected continuously at a flow rate of 2 ml/min. In these experiments the mucosal bath was oxygenated and stirred by a stream of humidified $O_2 - CO_2$. Fluxes were also measured during constant current clamping. Passing current through the epithelium leads to slow resistance changes (Frömter, 1972; Reuss & Finn, 1975*a*), the I/V plot being linear only for short current pulses. Due to additional diffusional delay J_{ms}^{Na} becomes constant only 15 to 25 min after constant current clamping. Steady-state fluxes were, therefore, measured for each period after at least 30 min had elapsed.

Results are given as the mean ± SEM; n = number of experiments.

Results

1) Measurement of the Luminal Membrane Potential and the Intracellular Sodium Activity

The potential change recorded with the sodium electrode after impalement of cells from the mucosal side is composed of two components,

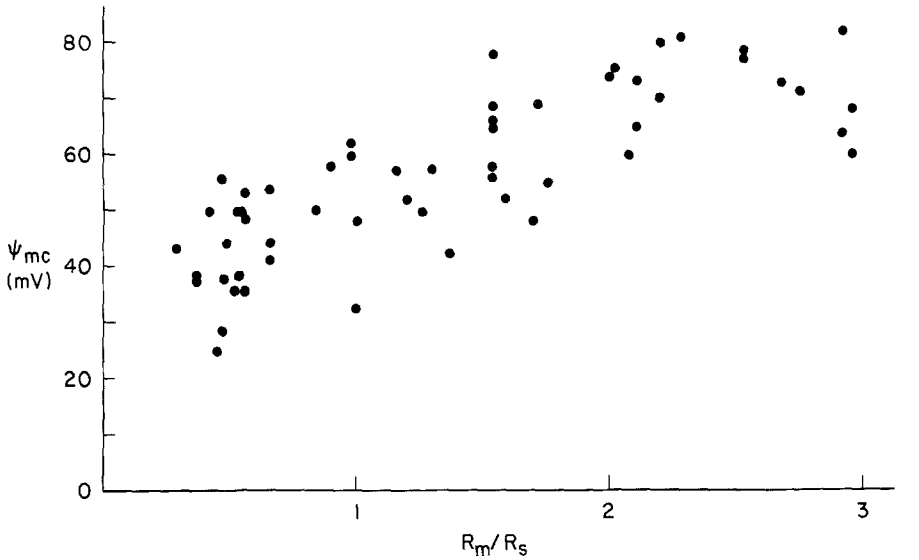

Fig. 3. Relationship between voltage divider ratio (r) and the luminal cell membrane potential (Ψ_{mc}) obtained from random impalements in 5 *Necturus* gallbladders. Only potential readings stable within 1 mV for longer than 1 min were accepted. These were most frequently obtained when the impalement resulted in a step voltage change and not in a transient overshoot or gradual increase. After some impalements a spontaneous decrease of Ψ_{mc} and the voltage divider ratio occurred. Further advancing of the electrode led to stabilization of Ψ_{mc} and r, unless apparent touching of the contraluminal membrane from the inside and its possible damage led to a step or gradual decrease of the intracellular potential

the change of the sodium potential from the extracellular to the intracellular value (E_{Na}) and the transmembrane electric potential difference (Ψ_{mc}). The intracellular sodium activity, $[Na]_i$, is evaluated from E_{Na} after correction for Ψ_{mc}. One way to obtain the reference transmembrane potential was to impale and to record potential differences from nearby cells with a second microelectrode of simular tip size (resistance between 3–10 MΩ, tip potentials <2 mV) as the sodium electrode. As summarized in Fig. 3, and as observed by other investigators (Frömter, 1972; Reuss & Finn, 1975*a*; van Os & Slegers, 1975), a considerable range of luminal membrane potential values was found. Differences in Ψ_{mc} as large as 15 mV were recorded with two Ling-Gerard Microelectrodes even in electrically coupled adjacent cells. Similarly, the sodium electrode measured stable values of $\Psi_{mc}-E_{Na}$ over a range of 37 to 128 mV.

Since this large variability of intracellular potentials could be due to damage of the luminal membrane during impalement, we passed current pulses through the epithelium and recorded the voltage divider ratio, r,

as a measure of the luminal membrane resistance. Figure 3 summarizes the relationship between the luminal membrane potential and the voltage divider ratio. It is apparent that a low relative luminal membrane resistance is generally associated with a low membrane potential. This dependence of Ψ_{mc} on the voltage divider ratio may be explained both by intrinsic variability of the luminal membrane resistance as well as by damage of the cell membrane by the recording electrode (*see Appendix*).[1] Suzuki and Frömter (1977) have recently reported similar observations.

Since a similar explanation is most likely to hold for the large variability of the potential measured by the sodium-electrode ($\Psi_{mc} - E_{Na}$), it was desirable to evaluate Ψ_{mc} for the same cell where $[Na^+]_i$ was to be measured. The use of double-barrelled sodium-sensitive microelectrodes would inevitably have led to larger tip sizes and increasing damage to the cell membrane. Advantage was, therefore, taken of the biphasic time course of the potential change when the tip of the sodium electrode traverses the cell membrane and becomes exposed either to the intracellular sodium concentration upon impalement or the extracellular solution after withdrawing the electrode. An initial step change of the potential was regularly followed by a second slow phase, the first measuring Ψ_{mc}, the second E_{Na}. The delay in reaching the second

[1] Frequently, low and unstable luminal membrane potentials associated with a low value of the voltage divider ratio were recorded immediately after puncturing the cell. In some instances further advancing of the microelectrode into the cell led to an increase of Ψ_{mc} and r and sometimes to stabilization of these parameters. As a typical example, the following pairs of values (Ψ_{mc}; $R_m/(R_m+R_s)$, fractional resistance of the luminal membrane) were obtained immediately after advancing the microelectrode by 5 μm steps into a cell: 7/0.07; 25/0.21; 37/0.34; 49/0.62. An increase of the intracellular potential measured by advancing the microelectrode into the cell was also observed by Zeuthen (1976, 1977). He interpreted this finding by postulating the existence of a significant intracellular potential gradient. This explanation seems unlikely, and similar views have been advanced by Suzuki and Frömter (1977). By two-dimensional cable analysis the resistance across the luminal and serosal membrane was determined to be 4.5 and 2.9 kΩ cm^2, respectively (Frömter 1972; Reuss & Finn 1975*a*). In contrast, studies of horizontal current spread within the epithelial cell layer yield a resistivity of 4.1 kΩ cm (this value is calculated from the data of Frömter for an epithelial thickness of 40 μm and it includes the intercellular coupling resistance). If the observed variance of the voltage divider ratio were due to incidental and different locations of the electrode tip along a presumed high intracellular resistance this would have to amount to half the sum of R_m and R_s (the range of r from 0.3 to 3.0 in Fig. 3 reveals fractional resistances, $R_m/(R_m+R_s)$, from 0.25 to 0.75). For a cell height of 40 μm this would give a cytoplasmic resistivity of 0.9 MΩ cm ($(4.5+2.9)\times 0.5$ KΩ cm$^2/4\times 10^{-3}$ cm). In view of this excessively high value, it is therefore concluded that the voltage divider ratio is determined by membrane properties only, and that, in our study, low potential readings are due to leaky impalements and variability of R_m (*see Appendix*). Advancing of the microelectrode after leaky impalements might facilitate sealing of the cell membrane around the electrode shaft.

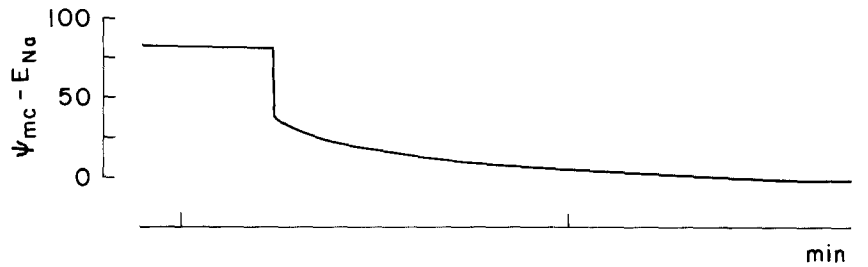

Fig. 4. Typical trace of the potential change recorded during withdrawal of a sodium-sensitive glass microelectrode from a cell after intracellular equilibration. The step change (within 3 sec) reflects the membrane potential; the slow potential change is due to the exposure of the sodium-sensitive glass membrane to the solution in the recess of the tip which slowly equilibrates with the extracellular fluid

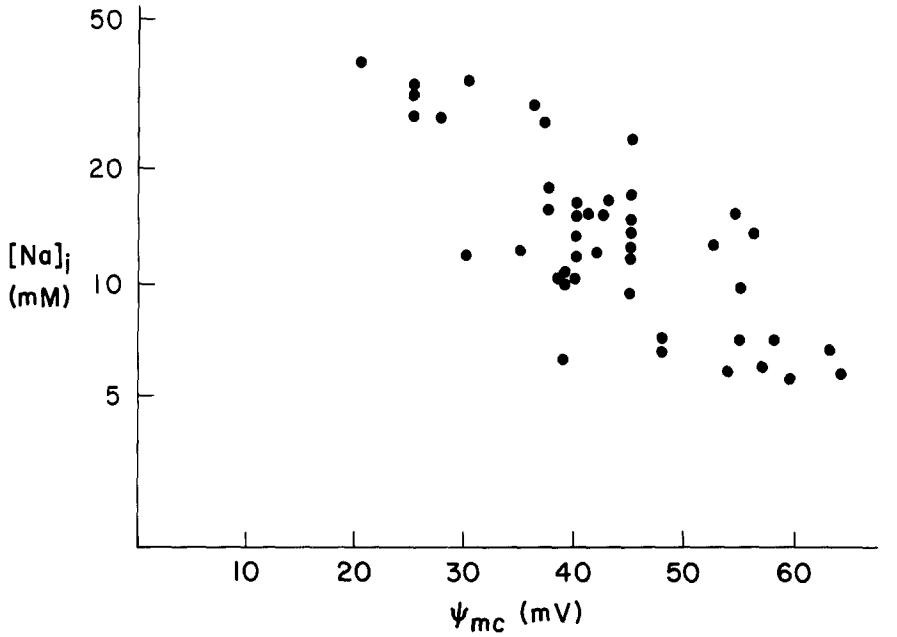

Fig. 5. Relationship between the luminal membrane potential (Ψ_{mc}) and the intracellular sodium activity $[Na^+]_i$, (logarithmic scale) obtained by analyzing potential changes recorded during withdrawal of the sodium electrode after intracellular stabilization

potential level is due to the slow equilibration between the intracellular fluid and the extracellular fluid in the recess of the sodium-sensitive electrode tip. As seen in Fig. 4, after intracellular equilibration has been achieved, the same biphasic response is observed when the electrode is withdrawn from the cell and exposed to the different extracellular sodium concentration.

Data obtained by this method are summarized in Fig. 5. Similar to the relationship between luminal membrane potential and the voltage divider ratio, a wide range of intracellular sodium activities was found and the magnitude of the membrane potential and the intracellular sodium concentration were correlated ($r=0.74$): a low Ψ_{mc} was found to be associated with a high $[Na^+]_i$. According to the above considerations, a leak in the puncture site should lead to an increase of $[Na^+]_i$ and probably a loss of intracellular K. This, in turn, may contribute to the decrease of the measured luminal membrane potential which is known to be K^+-dependent (Reuss & Finn, 1975*b*, van Os & Slegers, 1975). It seems, therefore, reasonable to assume that low potential recordings have doubtful physiological significance, and we have chosen to exclude them. Choosing lower limits of Ψ_{mc} of 40 mV, the mean values obtained from the data in Fig. 5 were, for control conditions, $\Psi_{mc}=48.0 \pm 1.3$ mV and $[Na^+]_i=12.1 \pm 4.6$ mM ($n=29$). A lower limit of Ψ_{mc} of 50 mV gives corresponding values of $\Psi_{mc}=57.6 \pm 2.7$ mV and $[Na]=9.2 \pm 3.8$ mM ($n=11$).

In the following experiments luminal bathing solutions were varied during recording with two cellular microelectrodes. Changes of $[Na^+]_i$ were evaluated from the mean changes of Ψ_{mc} and $(\Psi_{mc}-E_{Na})$, recorded with separate Ling-Gerard and sodium-sensitive electrodes, respectively.

2) Dependence of the Intracellular Sodium Activity on the Electrochemical Potential Gradient across the Luminal Cell Membrane

The purpose of these experiments was to study the change of the intracellular sodium activity under a condition where diffusional entry of sodium across the luminal membrane is suddenly abolished. Since the luminal membrane is permeable to both Na and K, although preferentially permeable to potassium ions (Reuss & Finn, 1975*b*, van Os & Slegers, 1975), replacement of luminal Na^+ by K^+ results in a simultaneous decrease of the luminal membrane potential difference (Ψ_{mc}) and the chemical potential difference for sodium (E_{Na}), the latter reversing its polarity when $[Na^+]_o<[Na^+]_i$. As can be seen from inspection of Fig. 6 where the initial electrical events are depicted, sodium equilibrium ($\Psi_{mc}-E_{Na}=0$) was approached when 90 mM Na^+ was replaced by K^+, to give a concentration of 92.5 mM K^+.

After abolishing the electrochemical potential difference of sodium across the luminal membrane, the further time course of the change of

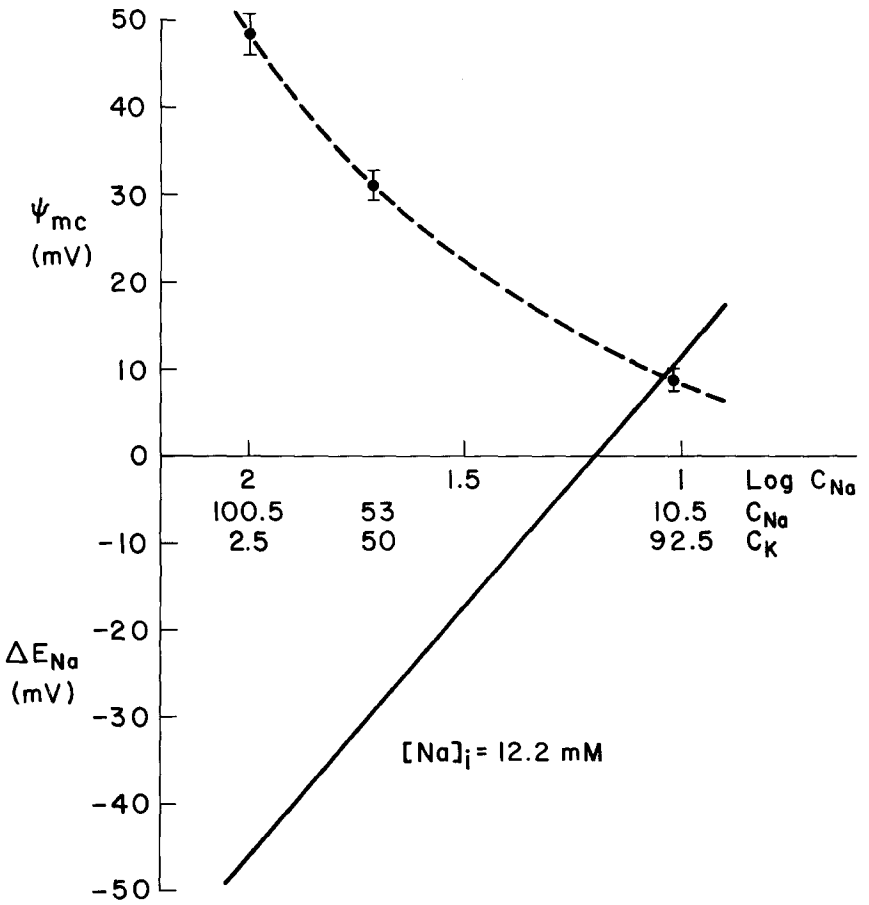

Fig. 6. Changes of the luminal membrane potential (Ψ_{mc}) as a function of the extracellular sodium and potassium concentrations, C_{Na} and C_K. Recorded values of Ψ_{mc} are compared to the calculated chemical sodium gradient ($[Na^+]_i = 12.2$ mM) across the cell membrane assuming no initial rapid changes of $[Na]_i$ when the ion concentrations of the luminal bathing solution were varied. Their difference ($\Psi_{mc} - E_{Na}$) is equal to the driving force for diffusional entry of sodium into the cell. This difference approaches zero when 90 mM sodium are replaced by potassium

$[Na^+]_i$ was analyzed as depicted in Fig. 7. $\Psi_{mc} - E_{Na}$ rose at an initial rate of 2.5 mV/min while Ψ_{mc} remained constant, showing that $[Na^+]_i$ decreased. Calculated mean values of $[Na^+]_i$ were 12.5 mM during perfusion with control solution and 11.7 mM immediately after the ionic shift. Subsequently, sodium activity decreased at an initial rate of 9.5%/min. After 30 min perfusion with the low Na^+-high K^+ solution in the luminal bath, a significant sodium gradient built up again. At that time a new steady-state value of Ψ_{mc} (8.1 ± 1.6 mV) and of $[Na^+]_i$ (3.5 ± 0.2 mM, $n = 5$) was obtained.

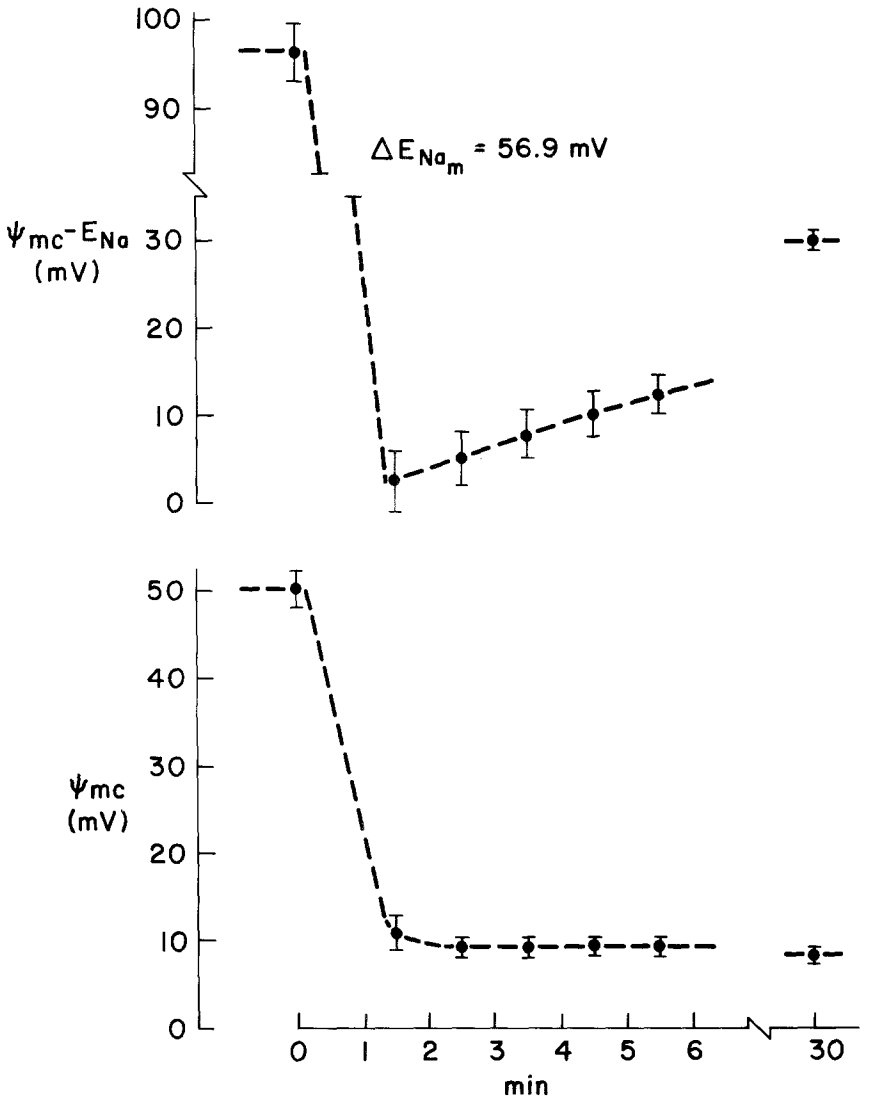

Fig. 7. Changes of Ψ_{mc} and $(\Psi_{mc} - E_{Na})$ recorded during a shift of the luminal bathing solution from 100.5 mM Na, 2.5 mM K to 10.5 mM Na and 92.5 mM K. Mean values ± SEM of 6 simultaneous records with a Ling-Gerard and a sodium-sensitive electrode. Note that diffusion equilibrium across the luminal membrane ($\Psi_{mc} - E_{Na} \simeq 0$) is obtained by this ionic shift. The following decrease of $[Na^+]_i$ (rise of E_{Na}) reflects the rate of antiluminal sodium extrusion

The initial change of $[Na^+]_i$ by 1.1 mM/min amounts to a sodium efflux of 93 pmol/cm^2 (calculated for the volume of an epithelial sheet of 1 cm^2 and a thickness of 40 μm and an assumed intracellular activity coefficient of 0.78). From the data of van Os and Slegers (1975) it seems probable that the basolateral cell membrane is only very sparingly

permeable to sodium ions. One may, therefore, assume that the above calculated flux represents a minimal estimate of the rate of active sodium translocation across the basolateral cell membrane. Two points should be considered. First, since the sodium electrode measures changes of the sodium activity with some delay, only a lower limit of the initial change of $[Na^+]_i$ can be estimated. Second, nonionic entry of sodium into the cell across the luminal membrane, albeit reduced at the low extracellular sodium concentration, could provide an additional sodium supply for the pump. Provided that the basolateral pumping rate does not appreciably change by the ionic shift in the luminal bathing solutions, this calculated flux would also obtain under control conditions. Disregarding other mechanisms of sodium entry across the luminal membrane than diffusion, a sodium conductance (g_{Na}) of 93×10^{-6} mho/cm^2 at the normal driving force of 96 mV would be necessary to accommodate this flux.[2]

In the following experiments, an independent estimate of the sodium conductance of the luminal membrane was obtained by analyzing the circuit parameters of the epithelium (Fig. 2). It will become apparent that the obtained luminal NA conductance value (12.3×10^{-6} mho/cm^2) is low enough to suggest that diffusion is not the only mechanism by which sodium enters the cell from the lumen.

3) Effects of Changes of the Luminal Ion Concentrations on Electrical Parameters of the Epithelium

Luminal membrane potential (Ψ_{mc}), the transepithelial potential (Ψ_{ms}) and the transepithelial resistance (R_{te}), and the voltage divider ratio ($r = R_m/R_s$) were recorded continuously during isotonic substitution of luminal NaCl (90 mM) by KCl or raffinose. The data were analyzed on the basis of the equivalent circuit shown in Fig. 2 following the method of Reuss and Finn (1975*b*). Estimates of the electromotive forces across the luminal (mucosal) (E_m) and basolateral (serosal) (E_s) can be obtained for control conditions by this procedure, and changes of E_m and of the E_{ms} of the lateral paracellular shunt (E_L) can be evaluated after ionic substitutions.

These calculations rely on assumed values of the emf across the shunt (E_L) and on an estimate of the resistance of the basolateral cell mem-

[2] The sodium chord conductance of the luminal membrane was calculated by $I_{Na} = J_{Na} F = g_{Na}(\Psi_{mc} - E_{Na})$ (5), where I_{Na} is the sodium current per unit area, J_{Na} is the sodium flux per unit area, F the Faraday, g_{Na} the specific membrane conductance for sodium, ψ_{mc} the luminal membrane potential, and E_{Na} the chemical potential difference for Na across the luminal membrane.

Table 1. Summary of electrical parameters obtained in *Necturus* gallbladder after ionic substitutions in the mucosal bath and after amphotericin B

	ψ_{mc} (mV)	ψ_{cs} (mV)	ψ_{ms} (mV)	R_{te} (Ω cm^2)	R_m/R_s
I. Control ($n=12$) (2.5 K, 100.5 Na)	61.5±3.3	−63.0±3.4	−1.5±0.3	177±7	1.49±0.17
High K ($n=12$) (92.5 K, 10.5 Na)	11.2±0.8	−30.9±1.6	−19.7±1.4	158±9	0.47±0.04
II. Control ($n=4$) (2.5 K, 100.5 Na, 98.1 Cl)	74.9±4.4	−76.0±4.5	−1.1±0.1	126±6	2.14±0.42
Raffinose ($n=4$) (2.5 K, 10.5 Na, 8.1 Cl)	96.3±4.6	−70.6±4.7	25.7±0.1	217±9	3.29±0.78
III. Control ($n=8$)	51.4±3.1	−53.1±3.2	−1.7±0.3	176±19	1.45±0.29
Amphotericin B ($n=8$) (10 µg/ml)	7.3±0.8	−14.4±1.3	−7.1±0.6	171±17	0.10±0.02

brane (R_s). For control conditions with symmetrical luminal and serosal bathing media E_L will be close to zero. R_s has been calculated by cable analysis to be 2.9 kΩ cm^2 (Frömter, 1972; Reuss & Finn, 1975*a*). The resistance of the luminal membrane (R_m) and of the shunt (R_L) were calculated by Eqs. (3) and (4) and E_m and E_s by Eqs. (1) and (2), assuming E_L is zero. The changes of E_m, E_L, and R_L after the ionic substitutions were calculated by the same set of equations and assuming the E_s and R_s are not altered by ion concentration changes in the mucosal bathing solution.

As can be seen in Table 1 and Fig. 8, replacement of luminal Na^+ by K^+ led to the immediate depolarization of the cells, the lumen negative transepithelial potential increased and the voltage divider ratio and the transepithelial resistance were reduced. Figure 9 shows results from a raffinose substitution experiment. After substitution of luminal NaCl by raffinose, Ψ_{mc} was immediately hyperpolarized, the transepithelial potential was shifted to a lumen positive value, and the voltage divider ratio and the transepithelial resistance increased. The basolateral membrane potential (Ψ_{cs}) depolarized slowly at a rate of 7.1±1.1 mV/min.

The results summarized in Tables 1 and 2 are in good agreement with those obtained by Reuss and Finn (1975*b*) employing other ion substitution experiments. They show that the emf of the shunt pathway (E_L) is the main determinant of the transepithelial potential (Ψ_{ms}) after ionic substitutions. From the observed transepithelial potential changes after substitution of K for Na and of raffinose for NaCl in the mucosal

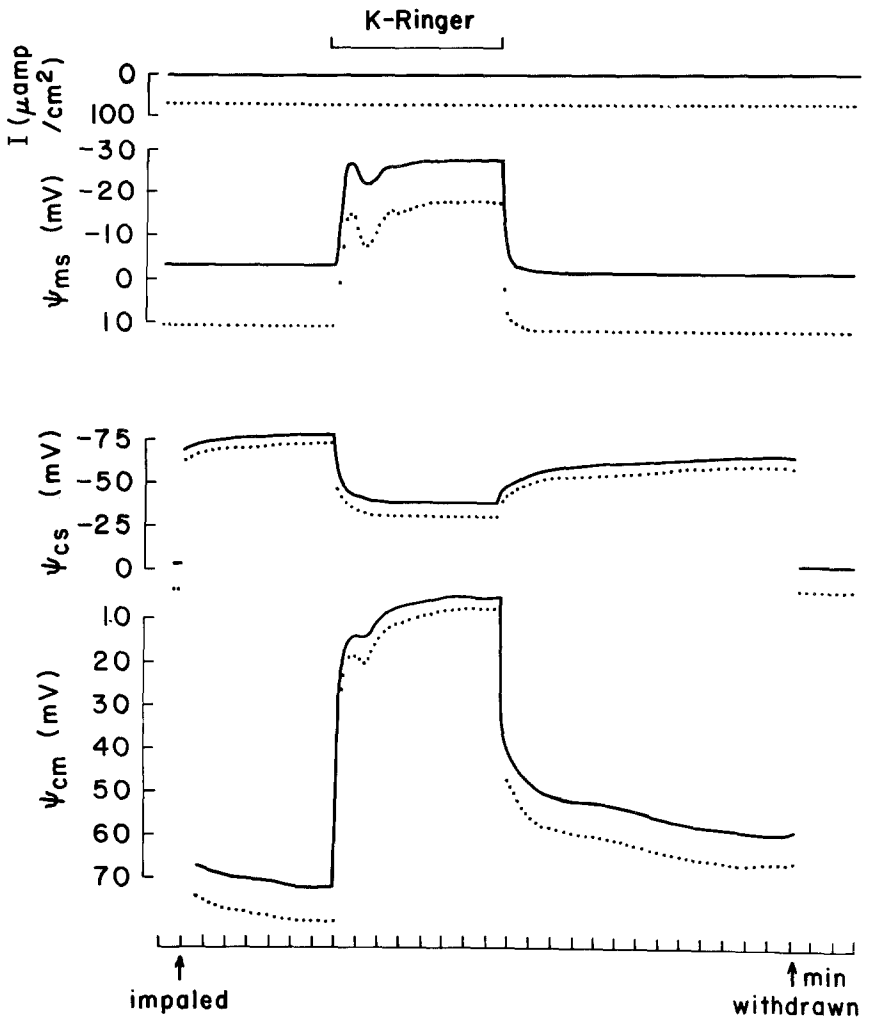

Fig. 8. Continuous record of potential changes measured across the whole epithelium (Ψ_{ms}) and across the serosal (Ψ_{cs}) and mucosal (Ψ_{mc}) cell membrane during a shift from 100.5 mM Na^+, 2.5 mM K^+ to 10.5 mM Na^+, 92.5 mM K^+ luminal bathing solution. Note the decrease of the transepithelial and mucosal membrane resistance during exposure to high K-Ringer revealed by the decrease of the amplitude of short potential deflections of Ψ_{ms} and Ψ_{mc} due to transepithelial current pulses (upper trace)

solutions, a permselectivity of the shunt pathway of $P_K > P_{Na} > P_{Cl}$ can be deduced. It can also be shown that the luminal membrane resistance, on the other hand, plays a key role in determining Ψ_{mc} under the influence of E_L and E_s such that a decrease of E_m is obtained after luminal replacement of NaCl by raffinose despite the fact that Ψ_{mc} increases. E_m decreases also after a luminal substitution of Na^+ by K^+. The data

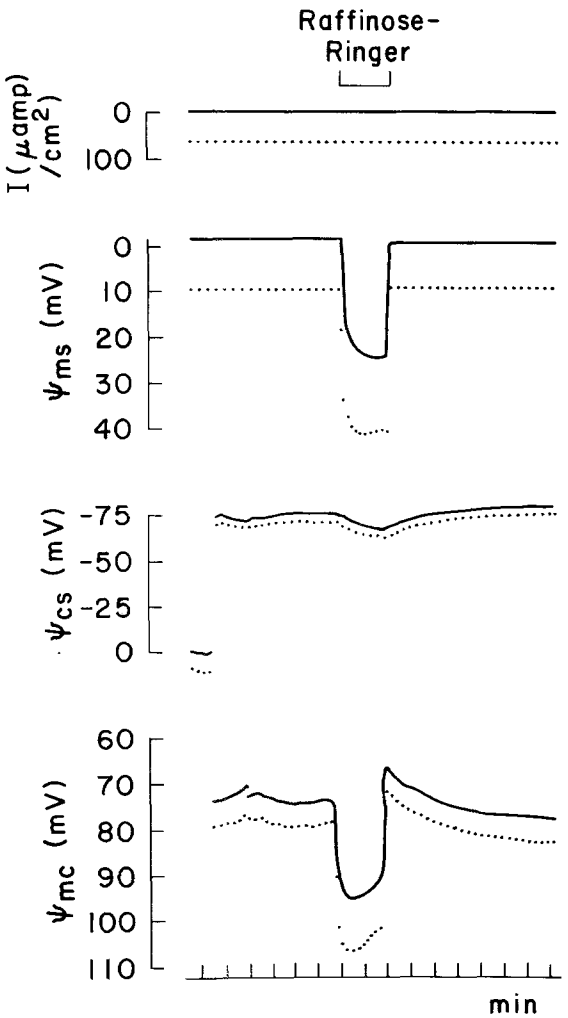

Fig. 9. Record as in Fig. 8, but showing the effects of replacement of 90 mM NaCl by raffinose in the luminal bathing solution

indicate a permselectivity of the luminal membrane for conductive fluxes of $P_K > P_{Cl} > P_{Na}$.

For evaluation of individual ion permeabilities of the paracellular shunt pathway the Goldman-Hodgkin-Katz-equation was used to define its emf (E_L). The following relative ion permeabilities were obtained from the values of E_L given in Table 2: $P_{Na}/P_K = 0.436$, $P_{Cl}/P_K = 0.085$. Relating conductances (g_i) to permeabilities (P_i) by the relationship $g_i = P_i C_i F^2/RT$ and using individual ion concentrations in control conditions (C_i) yields the following transference number ratio: $t_{Na}:t_K:t_{Cl} = 0.80:0.05:0.15$.

Table 2. Summary of calculated circuit parameters based on the values in Table 1[a]

	R_m (Ω cm^2)	R_s (Ω cm^2)	R_L (Ω cm^2)	E_m (mV)	E_s (mV)	E_L (mV)
I. Control	4309	(2900)	181.5	25.9	−87.0	(0)
High K[c]	1366	(2900)	164.1	−15.2	(−87.0)	−16.5
II. Control	6206	(2900)	128.0	21.6	−100.9	(0)
Raffinose[d]	9547	(2900)	220.7	−3.5	(−100.9)	28.0
III. Control	4217	(2900)	180.5	11.7	−80.4	(0)
Amphotericin B	302	(2900)	180.6	−4.6	−128.4	(0)

[a] The value of R_s is taken from Frömter, 1972[b]. E_L is assumed to be zero when the mucosal and serosal bathing solutions have identical ionic compositions.

[b] The use of other published values of R_m and R_s (Frömter, 1972; Reuss & Finn 1975) would have led to only slightly different estimates of E_m and E_s since the reported values of the voltage divider ratio are quite comparable to ours.

[c] $\Delta E_{Na} = 56.9$ mV; $\Delta E_K = 91.0$ mV.

[d] $\Delta E_{Na} = 56.9$ mV; $\Delta E_{Cl} = 62.8$ mV.

The determination of ion conductances of the luminal cell membrane suffers from lack of knowledge of intracellular ion concentrations other than $[Na^+]_i$. A rough approximation may be obtained though by relating changes of the emf across the luminal membrane (ΔE_m) to changes of the chemical potential of the individual ions (ΔE_i) in the luminal bathing solution by $\Delta E_m = \Sigma t_i \Delta E_i$ for the two substitution experiments summarized in Tables 1 and 2. It is recognized, however, that t_i may vary with the respective ion concentrations and the membrane potential. Limits of the transference numbers were obtained by solving the equations:

$-41.1 = 56.9\, t_{Na} - 91.0\, t_K$ for Na^+ substitution by K^+, and

$-25.1 = 56.9\, t_{Na} - 62.8\, t_{Cl}$ for NaCl substitution by raffinose

(*see* legend of Table 2 for relevant numerical values).

Assuming $t_{Na} + t_K + t_{Cl} = 1$, gives $t_{Na}:t_K:t_{Cl} = 0.06:0.49:0.45$, and for $R_m = 4.78$ kΩ cm^2 (mean control value of ion substitution experiments in Table 2), the ion conductances are $g_{Na} = 12.3$, $g_K = 102.1$, $g_{Cl} = 94.7$ μmho/cm^2.

These values seem reasonable when they are compared with the changes of the luminal membrane resistance observed during these ion substitutions (*see* Table 2). This is apparent from the decrease of the luminal membrane resistance, R_m, upon luminal substitution of sodium by potassium. The sharp decrease of this value from 4.31 to 1.37 kΩ cm^2

is consistent with a large contribution of g_K to the luminal membrane conductance compared to g_{Na}. Alternatively, the increase from 6.21 to 9.55 kΩ cm^2 observed upon replacement of luminal NaCl by raffinose indicates a significant contribution of g_{Cl} to the luminal membrane conductance.

4) Effects of Amphotericin B on Electrical Parameters and Intracellular Sodium Activity

Amphotericin B was applied in the luminal bathing solution in a concentration of 10 μg/ml, and electrical parameters of the epithelium and the intracellular sodium activity were measured as described.[3] The transepithelial potential rose within 2 to 5 min by as much as 15 mV (lumen negative), the epithelial cells were rapidly depolarized and the luminal membrane resistance decreased, while the transepithelial resistance showed initially only insignificant changes. These data are summarized in Tables 1 and 2, and results from an individual experiment are shown in Fig. 10. During prolonged action of the drug a gradual decrease of the transepithelial potential difference and resistance was observed.

Circuit analysis (Fig. 2, *compare Results*, section *3*) of the data indicates that amphotericin B reverses the emf across the luminal membrane (E_m) and leads to an increase of the emf of the basolateral cell membrane (E_s), both effects accounting for the large increase of the transepithelial potential difference.[4] The reduction of R_m to 7% of its control value and the simultaneous reversal of E_m indicate that the luminal membrane loses its potassium selectivity and becomes highly permeable to sodium ions. This could also be shown by the change of the intracellular sodium activity. The recorded electrochemical potential difference ($\Psi_{cs} - E_{Na}$) decreased from 104.8 ± 8.9 to 15.3 ± 3.0 mV ($n = 5$)

[3] The commercially available solution contains desoxycholate, as stabilizer which had no effect on electrical parameters of the gallbladder when applied to the mucosal surface.

[4] Assuming that the effect of amphotericin B is primarily to reduce the luminal membrane resistance (R_m) and using Eq. (4) in the form of

$$\frac{1}{R_{te}} = \frac{1}{R_L} + \frac{1}{R_s(1+r)}$$

the resistance of the basolateral membrane (R_s) and the paracellular shunt (R_L) may be calculated (Lewis *et al.*, 1977) from the change of R_{te} and r given in Table 1 as 3015 and 180.3 Ω cm^2.

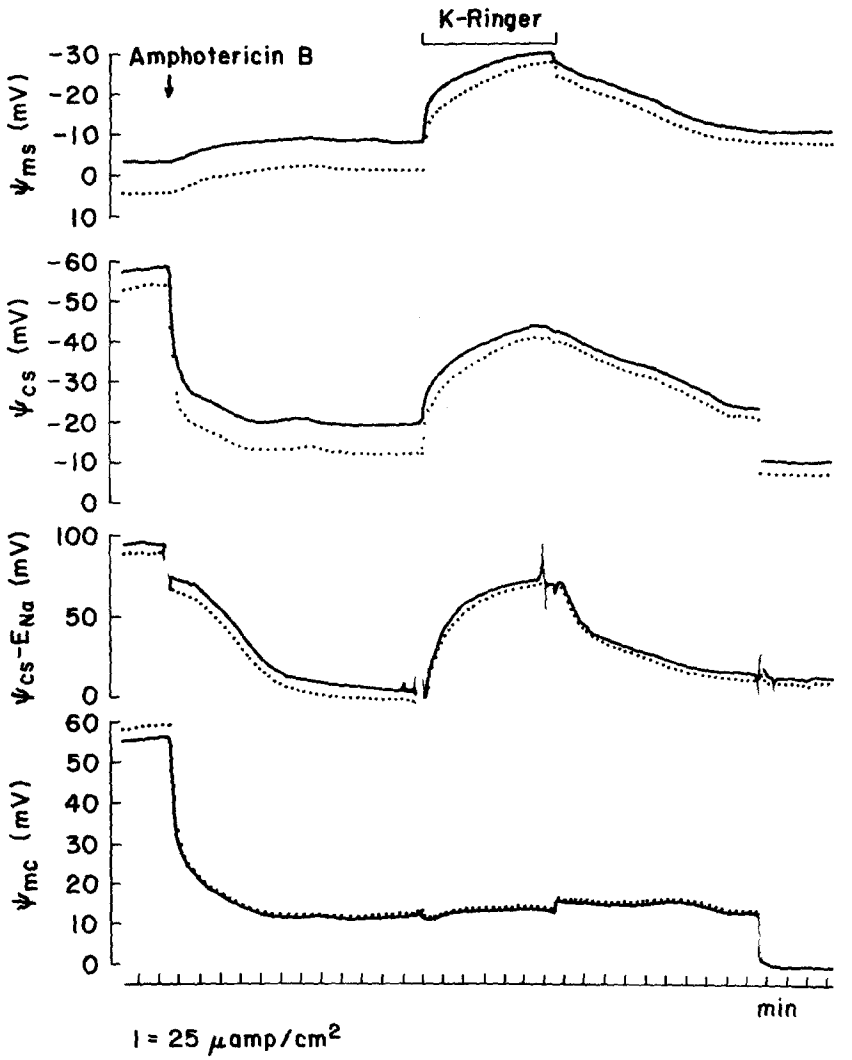

Fig. 10. Effects of luminal application of amphotericin B (10 μg/ml) and subsequent replacement of luminal Na^+ by K^+ on electrical parameters as in Fig. 8 but with an additional trace of the potential recorded with the sodium electrode ($\Psi_{cs}-E_{Na}$). Note the immediate depolarization of Ψ_{mc} with a concomittant decrease of the luminal membrane resistance (amplitude of deflections of Ψ_{mc}) and the rise $[Na^+]_i$ (depolarization of $\Psi_{cs}-E_{Na}$ compared to Ψ_{cs}) after application of amphotericin B, and the parallel change of Ψ_{cs} and Ψ_{ms} together with a fall of $[Na^+]_i$ after luminal replacement of Na^+ by K^+. The Ling-Gerard electrode was withdrawn at the end of the experiment

within 4 to 10 min, and $[Na]_i$ changed from 10.1 to 75.7 mM. The breakdown of the luminal membrane resistance could be further substantiated by the observation shown in Fig. 10, that luminal replacement of Na^+ by K^+, in the presence of amphotericin B, led to parallel changes

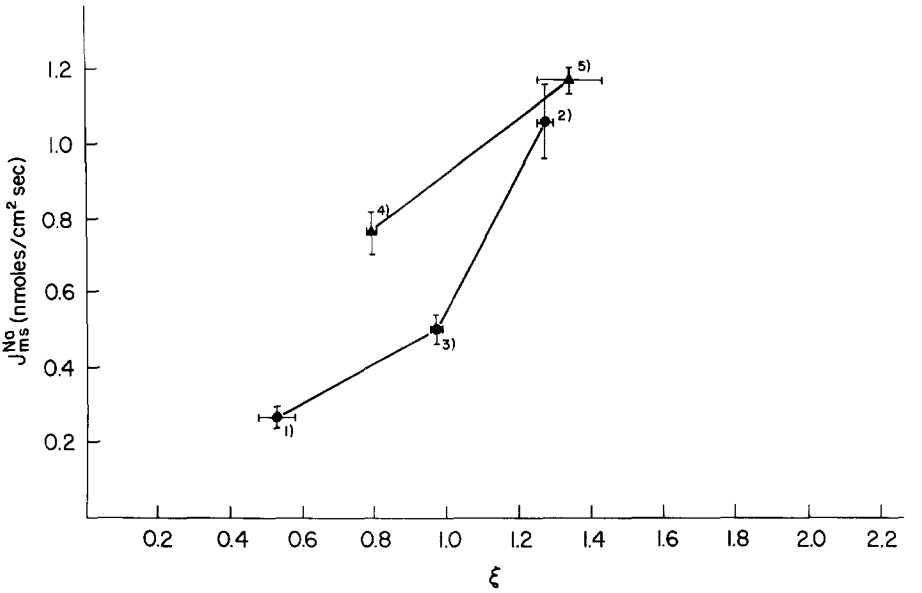

Fig. 11. Relationship between the electrical driving force (ξ) and the mucosa to serosa sodium flux during control conditions (dots) and after application of amphotericin B (triangles). Mean values $\pm$SEM; $n=5$. Experiments were carried out by applying the sequence of conditions: 1) current clamp, lumen negative; 2) current clamp, lumen positive; 3) spontaneous transepithelial potential; 4) spontaneous lumen negative potential after application of amphotericin B; 5) current clamp in the presence of amphotericin B, lumen positive. Measurements of the transepithelial conductance either by short current pulses or by shortly breaking the clamping current showed that the conductance was reduced at lumen negative potentials by a mean factor of 0.79 and increased at lumen positive potentials by 1.73. The conductance increased after lumen positive current clamping in the presence of amphotericin B by a factor of 1.30. Accordingly, the different slopes during lumen negative ($\xi < 1.0$) and lumen positive ($\xi < 1.0$) current clamping reflect changes in the transepithelial sodium permeability

of the transepithelial and basolateral potential differences. In these potassium substitution experiments, $[Na^+]_i$ approaches the luminal sodium concentration, and mean values 5 min after the ionic shift were: $[Na^+]_i = 23.3 \pm 0.4$ mM; $\Psi_{ms} = 29.7 \pm 0.3$ mV; and $\Psi_{cs} = -40.0 \pm 2.3$ mV ($n=3$).

5) Effects of the Transepithelial Voltage and of Amphotericin B on the Mucosa to Serosa Sodium Flux (J^{Na}_{ms})

The undirectional mucosa to serosa sodium flux and its voltage dependence were studied before and after addition of amphotericin B to the mucosal bath. Figure 11 shows a plot of the unidirectional sodium

flux against the transepithelial electrical driving force ($\xi = \Psi_{ms} F/RT$ $[1 - \exp(-\Psi_{ms} F/RT)]$ (Hodgkin & Katz, 1949). It is apparent that this plot is not linear, whereas Schultz and Zalusky (1964) and Desjeux, Tai and Curran (1974), for example, obtained a linear relationship for J_{sm}^{Na} as well as J_{ms}^{Na} in rabbit ileum. These authors were thus able to estimate the magnitude of a voltage independent cellular component of the respective fluxes by extrapolation to zero electrical driving force. For the present experiments in *Necturus* gallbladder the nonlinear relationship was not surprising since Frömter (1972) observed rectifying properties of this epithelium such that the application of lumen to serosa current increased the transepithelial conductance, whereas serosa to mucosa current decreased the conductance. The nonlinearity in our experiments suggests that the sodium permeability of the epithelium estimated from the slope of ξ against J_{ms}^{Na} is similarly voltage-dependent. It cannot be excluded, however, that voltage-dependent changes of the cellular component of the J_{ms}^{Na} contribute to the observed deviation from linearity. In view of this nonlinearity, it is not possible to estimate the active (nondiffusional) component of J_{ms}^{Na} from an intercept at zero electrical driving force. However, the observed increase of J_{ms}^{Na} by amphotericin B appears not to be associated with an increase in sodium permeability (slope of ξ *vs.* J_{ms}^{Na}) and, hence, must be due to a stimulation of active transcellular sodium transport.

Discussion

The present experiments were designed to analyze the mechanism of transcellular sodium transport across the gallbladder epithelium. Special emphasis was placed in our study on the role of intracellular sodium activity, the driving forces acting on sodium as it enters the cell from the lumen, and the problem of saturation of the active serosal sodium pump.

A mean intracellular sodium activity of 9–12 mM was found in gallbladder epithelial cells in control conditions. This value is significantly lower than that measured chemically in fish gallbladder (54 mM, Diamond, 1962), rabbit gallbladder (66 mM, Frizzell & Turnheim, 1978) or estimated indirectly for *Necturus* gallbladder ($\simeq$ 33.5 mM, van Os & Slegers, 1975). Our values are within the range of 12.9 to 46.3 reported by Zeuthen (1976) as measured with sodium-sensitive microelectrodes. Evidence presented in *Results* indicates our view that the lower sodium activities are more likely to be correct since they correspond to higher cell potentials and higher voltage divider ratios. Similar conclusions with

respect to the variability of the recorded membrane potential have recently been reached by Suzuki and Frömter (1977).

Transepithelial active sodium flux can be estimated by two approaches:

1) From the rate of decrease of the intracellular sodium activity in the absence of diffusional sodium influx across the luminal cell membrane (replacement of luminal Na^+ by K^+), a transport rate of 93 pmol/cm^2 sec can be calculated.

2) From the instantaneous short-circuit current, estimated from the transepithelial potential and conductance (control values in Table 1), a sodium flux of 88 to 101 pmol/cm^2 sec can be calculated.

Both values represent, however, minimum estimates of the magnitude of active transcellular transport (i) because of the delayed response of the recessed-tip sodium-sensitive electrode and (ii) since $I_{sc} < J_{act}^{Na}$ because of electroneutral entry of NaCl across the luminal membrane and a presumptive transcellular route of chloride absorption.

The electrochemical driving force acting on sodium across the luminal cell membrane can be directly assessed by the potential difference recorded with the sodium electrode in extracellular and intracellular position. Mean values range from 94.6 to 104.8 mV.

A sodium conductance of the luminal cell membrane of 12.3 μmho/cm^2 (determined in *Results*, section *3*) permits, therefore, diffusional entry of sodium across this membrane at a rate of 1.16 to 1.29 μA/cm^2 (12.1 to 13.4 pmol/cm^2 sec). This value is about 15% of the total active transepithelial sodium flux. These findings strongly suggest that additional mechanisms of influx of sodium across the luminal cell membrane exist.

A qualitatively similar conclusion was also reached by van Os and Slegers (1975) and by Reuss and Finn (1975*b*). These authors obtained resistance values of the luminal cell membrane of 4.13 and 3.35 kΩ cm^2, a permeability ratio of $P_{Na}/P_K = 0.37$, and ion conductance ratios of $t_{Na}/t_K = 0.15$, respectively; values in good agreement with those obtained by similar analysis in the present study (*see* Tables 1 and 2). Quantitative differences concern the use of higher values of $[Na]_i$ used in various calculations, and the finding of larger transepithelial sodium fluxes by these authors compared to approximately 100 pmol/cm^2 sec found in the present study and observed by K. Spring (*personal communication*). Therefore, estimates of diffusional entry of sodium accounted for 64% (van Os & Slegers, 1975) and <10% (Reuss & Finn, 1975*a*, *b*) of the transepithelial net flux. The cause of these differences in reported sodium

fluxes is not known. It is possible that seasonal variations, different bicarbonate concentrations of the bathing media (Gelarden & Rose, 1974), or different estimates of membrane area obtained by mounting the epithelium either stretched in a Ussing-type chamber or as a sac preparation, are involved. However, despite these quantitative differences, there is agreement with respect to the conclusion that the passive permeability of the luminal cell membrane of the gallbladder epithelium is too low to permit entry of sodium at a rate commensurate with active net transport.

It is likely that nondiffusional sodium entry proceeds by an electrically silent mechanism such as carrier-mediated neutral NaCl transport. Our data are consistent with a mechanism of coupled NaCl transport as suggested by earlier studies on fish, rabbit, and guinea pig gallbladders (Diamond, 1962, 1964, 1968; Wheeler, 1963, Dietschy, 1964) and with the findings in rabbit and guinea pig gallbladder that influx of Na^+ and Cl^- into the cell is partially dependent on the presence of the respective gegenion (Frizzell, Dugas & Schultz, 1975; Cremaschi & Henin, 1975). If such a mechanism is operative, the concentration gradient of sodium across the luminal membrane acts as a driving force for inward movement of sodium chloride. Charge neutralization by the carrier would facilitate chloride entry against an electrochemical gradient. It appears that the inherently low sodium conductance of the luminal cell membrane and the limited capacity of the additional sodium entry mechanism (carrier) are the rate-limiting steps of transepithelial sodium transport.

Evaluation of some kinetic properties of the sodium extrusion mechanism indicates that the sodium pump can operate against a steeper chemical activity gradient than normally encountered, and at higher transport rates as the load is increased. This conclusion is based on the following arguments.

When sodium entry across the luminal cell membrane is reduced by partial replacement of luminal Na^+ by K^+, a new steady state is reached. The cellular sodium activity falls from a control value of 12.5 to 3.5 mM. The pump now operates at a new steady-state level from cellular sodium activity of 3.5 mM against a serosal concentration of 100.5 mM. It is noteworthy that despite this change the electrochemical gradient established by the sodium pump across the serosal cell membrane changes little. The respective values are 98 mV in control and 109 mV after the decrease of Na_i and depolarization of the serosal cell membrane ($\Psi_{cs} = 30.9$ mV; $E_{Na} = 78$ mV).

Delivery of an increased load to the sodium pump was induced by

luminal application of amphotericin B. This amphipathic cyclic polyene antibiotic increases like nystatin chloride and sodium conductances of cholesterol containing thin lipid membranes by producing pores having an equivalent radius of 7 to 10.5Å (Andreoli & Monahan, 1968; Andreoli, Dennis & Weigl, 1969). A number of observations indicates that this compound increases sodium transport in epithelial membranes when added to the luminal bathing medium (Lichtenstein & Leaf, 1965; Bentley, 1968; Chen *et al.*, 1973; Frizzell & Turnheim, 1978). Evidence consistent with and supporting the view of stimulation by nystatin of electrogenic sodium extrusion across the antiluminal membrane has been reported by Lewis *et al.* (1977) in the rabbit urinary bladder and by Wills, Lewis and Eaton (1978) in the rabbit colon.

In rabbit and guinea pig gallbladder amphotericin B produces a sustained serosa positive transepithelial potential difference (Cremaschi *et al.*, 1977; Rose & Nahrwold, 1976) and a transient increase of O_2 consumption and sodium transport (Rose & Nahrwold, 1976). Only during prolonged drug exposure was a decrease of sodium transport observed (Cremaschi, Henin & Calvi, 1971*b*; Rose & Nahrwold, 1976). The stimulating effect on the transepithelial potential difference has been explained by an increase in sodium permeability of the luminal cell membrane (Cremaschi *et al.*, 1971*a*) as well as by activation or unmasking of rheogenic sodium pumping (Rose & Nahrwold, 1976). Amphotericin B effects similar to those in gallbladder epithelium have been reported for amphibian proximal and distal renal tubular epithelium (Wiederholt & Giebisch, 1974; Spring & Giebisch, 1977). Increased sodium transport and antiluminal electrical hyperpolarization were attributed to a rise in luminal cation permeability, enhanced rate of entry of sodium and stimulation of rheogenic sodium pumping across the basolateral cell membrane by an increase in cellular sodium concentration.

The present experiments fully support this view and provide, in addition, information on changes in cellular sodium activities during stimulation of sodium transport by amphotericin B. In our experiments luminal application of Amphotericin B led to rapid depolarization of the cells, a breakdown of the luminal membrane resistance, and a dramatic increase of intracellular sodium activities to almost extracellular values. The initial steep increase of the transepithelial potential (serosa positive) is thought to be partially due to reversal of the emf across the luminal cell membrane. This is in agreement with the observation of Reuss (1978) showing a larger increment of g_{Na} than of g_K. The sustained high value is

also quite consistent with the view that active basolateral rheogenic sodium pumping, estimated from the increase of the instantaneous short-circuit current (Table 1), and the unidirectional sodium flux (Fig. 11) proceeds at a fourfold higher rate as the intracellular sodium activity increases and the basolateral emf is augmented to 128 mV. Rheogenic sodium pumping has been considered to be the source of a substantial serosa positive transepithelial potential observed in gallbladders of goose, monkey, and man (Gelarden & Rose, 1974). The observation of a gradual decrease of the basolateral cell membrane potential after replacement of luminal NaCl by raffinose can be interpreted by a decrease of the rate of rheogenic sodium pumping across the antiluminal cell membrane due to the sharply diminished sodium load. Even if under control conditions a 1:1 coupled active Na−K transport alone were responsible for transepithelial sodium transport, it is likely that the coupling ratio is not fixed but increases as the load increases and the pump becomes current generating.

This work was supported by grants from the NIH (PCM 76-81674) and NSF (PHS-AM 17433). Dr. Graf received support from the Max Kade Foundation.

Appendix

Assessment of Impalement Damage

Simon A. Lewis and Jürg Graf

The phenomenon of impalement damage of an epithelial cell with a microelectrode will yield incorrect estimates of the individual cell membrane and junctional resistances as well as cell membrane potentials. This problem is accentuated when attempting to measure intracellular ion activities with ion specific microelectrodes (Lewis, Wills & Eaton, 1978). In order to feel confident about intracellular ion activity measurements, a criterion must be established which will allow the investigator to differentiate between damaged and nondamaged cells. Such a method was developed by Lewis *et al.* (1977). These authors used the polyene antibiotic nystatin to directly measure the amount of damage caused by microelectrodes. This technique, however, proves only to be useful for the so-called "tight" epithelia.

Recently Suzuki and Frömter (1977) demonstrated that microelectrodes with low resistance (large tips) resulted in a large scatter in the

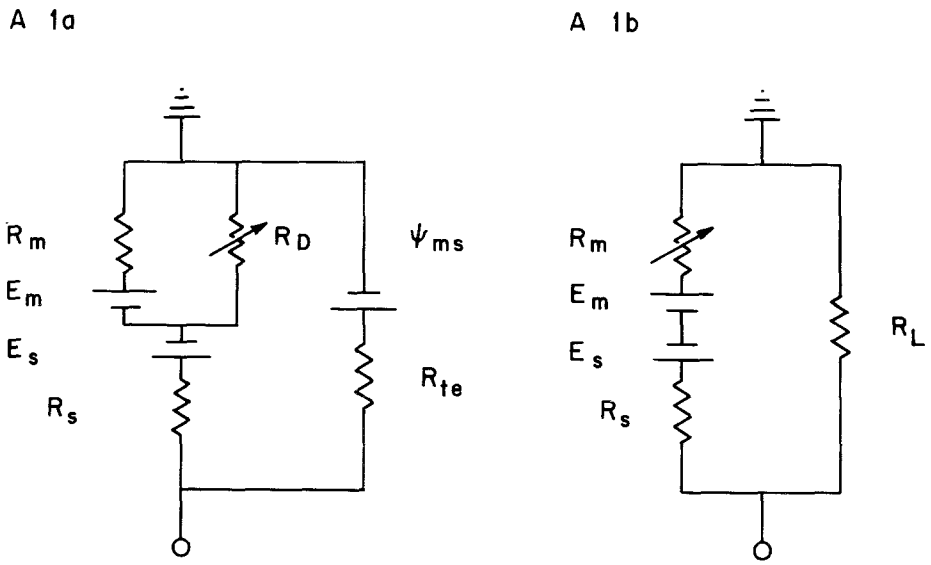

Fig. A1. (a): Equivalent circuit of the gallbladder for the case of microelectrode impalement damage. R_D is the parallel resistance introduced by the microelectrode. This resistor has a variable value which is dependent on the magnitude of damage. Other parameters are as described in Fig. 2. (b): Equivalent circuit of the gallbladder for the case of an intrinsically variable mucosal membrane resistance. Lettered parameters are the same as described in Fig. 2

fractional resistance measurements as well as mucosal membrane potential of the *Necturus* gallbladder. A plot of fractional resistance (r) *vs.* mucosal membrane potential of a single cell (Ψ_{mc}) indicated a near linear relationship with a zero intercept. Such a relationship is predicted by the equation:

$$\Psi_{mc} = r' \left(E_m \left(\frac{1}{r} - 1 \right) + E_s - \Psi_{ms} \right) \tag{A1}$$

where

$$r' = \frac{R_{md}}{R_{md} + R_s}$$

$$\left(\text{fractional resistance of a damaged cell where } R_{md} = \frac{R_m R_D}{R_m + R_D} \right)$$

$$r = \frac{R_m}{R_m + R_s} \text{ (fractional resistance of an undamaged cell).}$$

E_m and E_s are the electromotive force of the mucosal and serosal membranes, respectively, in a single cell. This equation is derived from

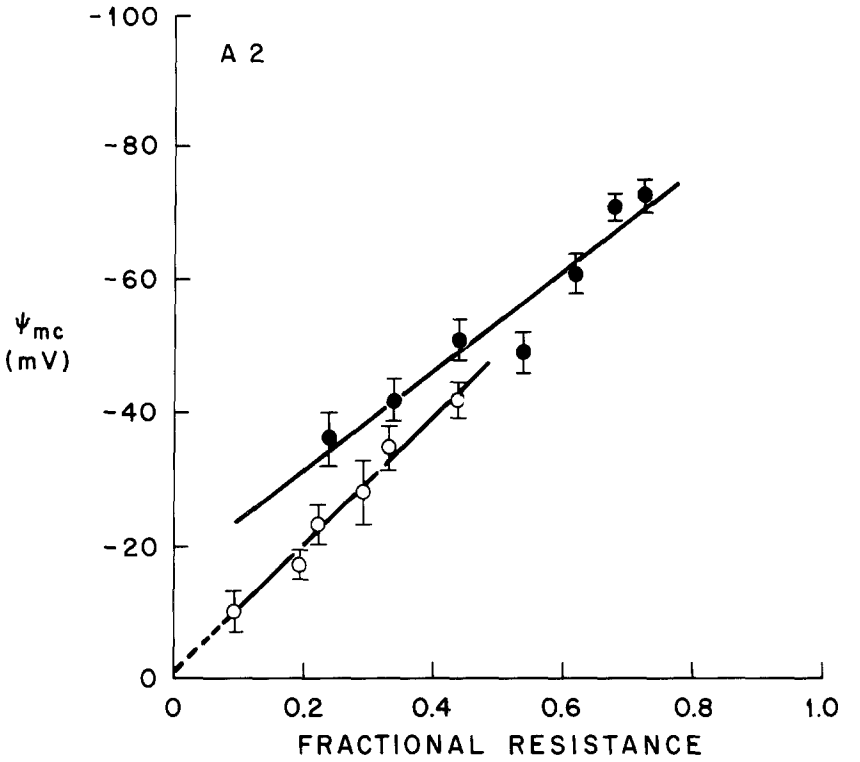

Fig. A2. Relationship between spontaneous mucosal membrane potential (Ψ_{mc}) (mucosal ground) and measured fractional resistance ($R_m/(R_m+R_s)$). Open circles (○) are collected data for unstable impalements with a linear regression $y=96x+0.8$ ($r=0.99$). Closed circles (●) are collected data for stable impalements with a linear regression $y=75x+16$ ($r=0.96$). Vertical bars are SEM

Fig. *A1a* on the assumption that impalement damage did not alter either E_m or E_s.

An alternate hypothesis for a large variation in fractional resistance is that it might reflect an intrinsic variability in the mucosal membrane resistance. Such a variability is described by the following equation (Fig. *A1b*) assuming R_m and $R_s \gg R_L$ [*see* Reuss & Finn, (1977) and Suzuki & Frömter (1977)].

$$\Psi_{mc}=(E_s-E_m)\,r+E_m \tag{A2}$$

which is a linear equation where a plot of Ψ_{mc} *vs.* r will have an intercept of E_m and a slope of E_m-E_s.

Figure *A2* demonstrates two sets of data. The open circles represent data in which the cellular impalements were unstable. Such data fit best

to a model which incorporates impalement damage as the factor responsible for variation in the fractional resistance [Eq. (A1)]. A linear regression analysis yields the equation $y=96x+0.8$. In addition, the closed circles represent collected data of stable impalements of Ψ_{mc} and fractional resistance, and a linear regression analysis yields the equation $y=75x+16.3$. In terms of Eq. (A2), we calculate an E_m value of 16 mV and an E_s value of 91 mV. These values are in excellent agreement with those of Reuss and Finn (1977) indicating that the variability of this data set is not necessarily a consequence of impalement damage, but might represent an intrinsic variability in membrane resistances.

These estimates of E_m and E_s in conjunction with Ψ_{ms}, R_{te} and a mean α (voltage divider ratio) values can be used to calculate values for R_m, R_s and R_L. Utilizing the equation,

$$\Psi_{ms}=\left(\frac{E_m-E_s}{R_m+R_s}\right)R_{te}=\left(\frac{E_m-E_s}{R_s(1+\alpha)}\right)R_{te}, \tag{A3}$$

where E_m and E_s are as previously described, $\alpha=1.54$, $\Psi_{ms}=2.0$ mV, and $R_{te}=171\,\Omega$ cm^2. R_s is calculated 2,020 Ω cm^2, R_m 3,040 Ω cm^2 and R_L of 177 Ω cm^2. These values again are in good agreement with those of Suzuki and Frömter (1977) and Reuss and Finn (1977).

We feel then that the large variability in fractional resistance at values of Ψ_{mc} greater than -40 mV is a consequence of an intrinsically variable mucosal membrane resistance and not a product of cell disruption, whereas that observed during unstable impalements may reflect cell damage.

References

Andreoli, T.E., Dennis, V.W., Weigl, A.M. 1969. The effect of amphotericin B on the water and nonelectrolyte permeability of thin lipid membranes. *J. Gen. Physiol.* **53**:133

Andreoli, T.E., Monahan, M. 1968. The interaction of polyene antibiotics with thin lipid membranes. *J. Gen. Physiol.* **52**:300

Bentley, P. 1968. Action of amphotericin B on the toad bladder: Evidence for sodium transport along two pathways. *J. Physiol. (London)* **196**:703

Brown, K.T., Flaming, D.G. 1974. Beveling of fine micropipette electrodes by a rapid precision method. *Science* **185**:693

Chen, L.C., Cuerrant, R.L., Rhode, J.E., Casper, A.G.T. 1973. Effect of amphotericin B on sodium and water movement across normal and cholera toxin-challenged canine jejunum. *Gastroenterology* **65**:252

Cremaschi, D., Henin, S. 1975. Na^+ and Cl^- transepithelial routes in rabbit gallbladder. *Pfluegers Arch.* **361**:33

Cremaschi, D., Henin, S., Calvi, M. 1971*a*. Transepithelial potential difference induced by amphotericin B and $NaCl-NaHCO_3$ pump localization in gallbladder. *Arch. Int. Physiol. Biochem.* **79**:889

Cremaschi, D., Henin, S., Calvi, M. 1971*b*. Inhibition of $NaCl-NaHCO_3$ pump by high levels of Na^+ salts in rabbit gallbladder epithelial cells. *Atti Accad. Naz. Lincei Rend.* **50**:216

Cremaschi, D., Henin, S., Meyer, G., Bacciola, T. 1977. Does amphotericin B unmask an electrogenic Na^+ pump in rabbit gallbladder? Shift of gallbladders with negative to gallbladders with positive transepithelial p.d.'s. *J. Membrane Biol.* **34**:55

Desjeux, J.F., Tai, Y.H., Curran, P.F. 1974. Characteristics of sodium flux from serosa to mucosa in rabbit ileum. *J. Gen. Physiol.* **64**:274

Diamond, J.M. 1962. The mechanism of solute transport by the gallbladder. *J. Physiol. (London)* **161**:474

Diamond, J.M. 1964. Transport of salt and water in rabbit and guinea pig gallbladder. *J. Gen. Physiol.* **48**:1

Diamond, J.M. 1968. Transport mechanisms in the gallbladder. *In:* Handbook of Physiology: Alimentary Canal. Vol. 5, p. 2451. American Physiological Society, Washington

Dietschy, J.M. 1964. Water and solute movement across the wall of the everted rabbit gallbladder. *Gastroenterology* **47**:395

Frizzell, R.A., Dugas, M.C., Schultz, S.G. 1975. Sodium chloride transport by rabbit gallbladder. Direct evidence for a coupled NaCl influx process. *J. Gen. Physiol.* **65**:769

Frizzell, R.A., Turnheim, K. 1978. Ion transport by rabbit colon: II. Unidirectional sodium influx and the effects of amphotericin B and amiloride. *J. Membrane Biol.* **40**:193

Fromm, M., Hegel, U., Beck, H., Weskamp, P. 1977. Effect of trypsin on DC and AC parameters of *Necturus* gallbladder epithelium. *Proc. Int. Union Physiol. Sci.* **13**:244

Frömter, E. 1972. The route of passive ion movement through the epithelium of *Necturus* gallbladder. *J. Membrane Biol.* **8**:259

Frömter, E., Diamond, J.D. 1972. Route of passive ion permeation in epithelia. *Nature, New Biol.* **235**:9

Gelarden, R.T., Rose, R.C. 1974. Electrical properties and diffusion potentials in the gallbladder of man, monkey, dog, goose and rabbit. *J. Membrane Biol.* **19**:37

Hodgkin, A.L., Katz, B. 1949. The effects of sodium ions on the electrical activity of the giant axon of the squid. *J. Physiol. (London)* **108**:37

Lee, C.O., Armstrong, W.McD. 1972. Activities of sodium and potassium ions in epithelial cells of small intestine. *Science* **175**:1261

Lewis, S.A., Eaton, D.C., Clausen, C., Diamond, J.M. 1977. Nystatin as a probe for investigating the electrical properties of a tight epithelium. *J. Gen. Physiol.* **70**:427

Lewis, S.A., Wills, N.K., Eaton, D.C. 1978. Basolateral membrane potential of a tight epithelium: Ionic diffusion and electrogenic pumps. *J. Membrane Biol.* **41**:117

Lichtenstein, N.S., Leaf, A. 1965. Effect of amphotericin B on the permeability of the toad bladder. *J. Clin. Invest.* **44**:1328

Os, C.H. van, Slegers, J.F.G. 1975. The electric potential profile of gallbladder epithelium. *J. Membrane Biol.* **24**:341

Reuss, L. 1978. Mechanism of transepithelial hyperpolarization produced by amphotericin B in *Necturus* gallbladder. *Biophys. J.* **21**:168*a*

Reuss, L., Finn, A.L. 1975*a*. Electrical properties of the cellular transepithelial pathway in *Necturus* gallbladder. I. Circuit analysis and steady-state effects of mucosal solution ionic substitutions. *J. Membrane Biol.* **25**:115

Reuss, L., Finn, A.L. 1975*b*. Electrical properties of the cellular transepithelial pathway in *Necturus* gallbladder. II. Ionic permeability of the apical cell membrane. *J. Membrane Biol.* **25**:141

Reuss, L., Finn, A.L. 1977. Mechanisms of voltage transients during current clamp in *Necturus* gallbladder. *J. Membrane Biol.* **37**:299

Rose, R.C., Nahrwold, D.L. 1976. Electrolyte transport by gallbladders of rabbit and guinea pig: Effect of amphotericin B and evidence of rheogenic Na transport. *J. Membrane Biol.* **29**:1

Schultz, S.G., Zalusky, R. 1964. Ion transport in isolated rabbit ileum. I. Short circuit current and sodium fluxes. *J. Gen. Physiol.* **47**:567

Spring, K., Giebisch, G. 1977. Kinetics of Na^+ transport in *Necturus* proximal tubule. *J. Gen. Physiol.* **70**:307

Suzuki, K., Frömter, E. 1977. The potential and resistance profile of *Necurus* gallbladder cells. *Pfluegers Arch.* **371**:109

Thomas, R.C. 1972. Intracellular sodium activity and the sodium pump in snail neurons. *J. Physiol. (London)* **220**:55

Thomas, R.C. 1976. Construction and properties of recessed-tip microelectrodes for sodium and chloride ions and pH. *In:* Ion and Enzyme Electrodes in Biology and Medicine. M. Kessler, L.C. Clark, Jr., D.W. Lübbers, I.A. Silver and W. Simon, editors. pp. 141–148. Urban & Schwarzenberg, Munich-Berlin-Vienna

Wheeler, H.O. 1963. Transport of electrolytes and water across the wall of rabbit gallbladder. *Am. J. Physiol.* **205**:427

Wiederholt, M., Giebisch, G. 1974. Some electrophysiological properties of the distal tubule of *Amphiuma* kidney. *Fed. Proc.* **33**:387

Wills, N., Lewis, S.A., Eaton, D.C. 1979. Active and passive properties of rabbit descending colon: A microelectrode and nystatin study. *J. Membrane Biol.* **45**:137

Zeuthen, T. 1976. Gradients of chemical and electrical potential in the gallbladder. *J. Physiol. (London)* **256**:32*P*

Zeuthen, T. 1977. Intracellular gradients of electrical potential in the epithelial cells of the *Necturus* gallbladder. *J. Membrane Biol.* **33**:281

Zeuthen, T., Monge, C. 1975. Intra- and extracellular gradients of electrical potential and ion activities of the epithelial cells of the rabbit ileum *in vivo* recorded by microelectrodes. *Philos. Trans. R. Soc. (London) B* **271**:277